All-Textile On-Body Metasurface Antenna

Esra Çelenk[1], * and Nurhan T. Tokan[2]

Abstract—In this work, a novel all-textile washable metasurface antenna is designed for WBAN/WLAN and mid-band 5G applications. Metasurface antenna is obtained by implanting SRR (Split Ring Resonator) metamaterials that show left-hand characteristics to the patch plane. The metamaterial arrays consisting of 4×1 and 4×2 SRRs are placed to lateral sides of a circular patch. The performance of the antenna is verified by a full-wave electromagnetic analysis tool. The results show that metamaterial arrays significantly increase gain and efficiency values of the circular patch antenna. Metasurface antenna consisting of 4×2 array of metamaterials increases the efficiency from 74% to 94.5% and the antenna gain from 6.81 dBi to 9.43 dBi. Performance of the antenna is observed on conformal surfaces, as well. An analysis is carried out to calculate the peak specific absorption rate on an arm phantom. Patterns of vertically bended antenna in $\varnothing = 0°$ and $90°$ planes and low SAR values up to 30 dBm input power proved suitability of the metasurface antennas for on-body applications. The antennas are fabricated by using standard textile manufacturing techniques. It was confirmed by the measurement results that the metasurface formed by the linear SRR arrays increases the antenna gain. With its low cost, fabrication with standard off-the-shelf parts, high gain, and efficiency features, the proposed antenna can be used in wireless body area networks and 5G applications.

1. INTRODUCTION

Wearable textile antennas are used in applications such as health monitoring, emergency rescue systems, physical education, military applications, public security, and location tracking [1, 2]. The textile material of the wearable antenna should have light weight and flexible form which makes the antenna easily integrated into clothing [3]. Felt, leather, fleece, and silk are widely used substrate materials of the textile antennas, whereas conductive textile is chosen as the conductor [4, 5]. Among the materials used as the dielectric in textile antenna, pure polyester has the lowest loss tangent [6, 7]. Smart textiles are designed to fit the body shape and ensure comfort for on-body usage [8, 9]. Wearable textile antennas are considered for Wireless Body Area Network (WBAN), Wireless Local Area Network (WLAN), and mid-band 5G applications, where data transmission at high data rates is provided [10, 12]. Technical problems such as antenna bandwidth, small size, and light weight have to be encountered for wearable antenna designs for 5G applications [13]. Narrow impedance bandwidth is a major problem in these antennas.

Manufacturing of the wearable antenna with standard textile fabrication techniques is important. Using standard off-the-shelf textile materials in the fabrication process reduces cost and time in production. Fabrication technique depends on the materials to be used, and it is a challenge to obtain required gain and size [11]. Recently, some examples based on automated processing of E-thread (Electronic thread) have been introduced as a solution to the manufacturing difficulties of textile antennas. E-threads have very good mechanical strength properties [14]. Conductive patterns are created on conductive E-textile materials by using laser cutting techniques [15].

Metasurfaces are two-dimensional variants of metamaterials that are nonexistent in nature. The electromagnetic properties of metamaterials are artificially produced [16]. Anomalous relative permittivity and relative permeability values such as low-positive or negative are observed within a certain frequency band [17–19]. Metasurfaces have many advantages in controlling the amplitude, phase, and polarization of the electromagnetic wave. They may be used to enhance the antenna gain [20]. Split-ring resonator (SRR) is the widely used unit element of a metasurface [21]. SRRs generate a left-handed medium that exhibits negative electrical permeability and magnetic permeability at the required frequency [22]. SRR metamaterial superstrate concept has been applied to microstrip patch antenna to obtain high gain and broad tunable frequency bandwidth [23, 24]. Although metamaterial structures in antenna design increase the antenna gain, their usage is not very common in textile antennas due to the difficulties experienced in production process. Thus, there are limited papers on all-textile antenna with metamaterials. An ultraminiaturized cavity-backed SIW all-textile antenna is designed using the metamaterial-inspired slot technique [25]. An all-textile and wearable wide-bandwidth planar inverted-F antenna including a metasurface is proposed [11]. A metasurface with high permittivity is placed above the antenna for size reduction and gain enhancement. A compact all-textile dual-band metamaterial-inspired patch antenna is proposed for WLAN applications [1]. The composite right/left-handed transmission loadings reduce the physical size of the antenna significantly. Conductive textile with low surface resistivity is used to fabricate the metallic layers [1, 11]. An embroidered metamaterial wearable monopole antenna that contains 2×2 electro-magnetic band gap matrix is proposed [26].

Usage of E-thread for the fabrication of metasurfaces in antenna design is not common in literature. Although E-thread is used for the manufacturing of antenna conductive layers in [14, 27, 28], the antennas do not contain metasurface. In this work, an all-textile, washable metasurface antenna is proposed for the use in textile applications. Restrictions of fabrication with E-tread are accounted in the design. This enables manufacturing of the conductor parts with embroidery machine using silver-plated highly conductive E-thread. Firstly, the circular patch antenna is designed. Then, different metasurface arrays consisting of 4×1 and 4×2 SRRs are placed on the antenna surface as given in Section 2. Radiation performances of the antennas are observed. On-body performance is investigated by the bended metasurface antennas. Performance comparison of planar and curved antennas is given in Section 3. Fabrication details and experimental characterization of the antennas are shown in Section 4. The Specific Absorption Rate (SAR) analysis is also carried out in Section 5. Section 6 concludes the paper.

2. ALL-TEXTILE ANTENNA AND METAMATERIAL SURFACE

On-body antennas are vital elements of health monitoring, emergency rescue, and tracking wireless applications. Manufacturing of all-textile on-body antennas by standard off-the-shelf parts reduces manufacturing complexity and enables simple and cost-effective mass production. Although E-textile has been considered as the conducting material of the textile antenna mostly, E-thread is introduced as an alternative. E-thread has good mechanical strength and facilitates with both planar and coplanar integration. In this work, silver coated E-thread is used for all conducting surfaces. Standard embroidery machine is used for prototyping of the antennas. By adding an array of metamaterial structures on the patch plane, a metamaterial surface is generated.

2.1. Metamaterial Unit Cell Design

SRR metamaterial structure was used in the design of the metasurface. Each SRR unit cell has $12.5 \, \text{mm} \times 12.5 \, \text{mm}$ (Length $\times$ Width) physical size. The width of the rings (t) is $1 \, \text{mm}$. The opening between rings is also $1 \, \text{mm}$. SRR unit cell is given in Figure 1. A polyester substrate with a thickness of $4 \, \text{mm}$, relative electrical permittivity of $\varepsilon_r = 1.9$ and loss tangent of $\delta_p = 0.0045$ (at $2.44 \, \text{GHz}$) is used. As the conducting material of the SRRs and antenna, Madeira HC-12 silver-coated conductive thread that can be embroidered and sewed on textile materials is used. It protects its electrical characteristics when being washed with mild detergent at $30°\text{C}$. Its resistance is smaller than $100 \, \Omega/\text{m}$ and offers high conductivity for electrical contacts and connections [29].

Dispersion characteristics of the SRR metamaterial unit cell are obtained. The boundary conditions
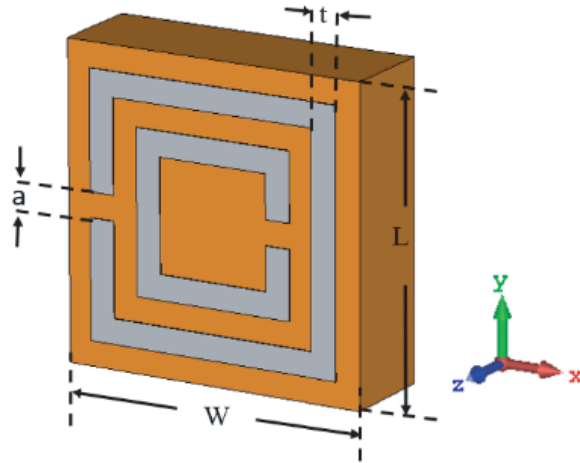
Figure 1. SRR unit cell.

are chosen as a perfect electric conductor (PEC) in x-axis and a perfect magnetic conductor (PMC) in z-axis. Full-wave analysis of the unit cell is carried out in HFSS, and scattering parameters below the diffraction frequencies are evaluated. PEC and PMC are characterized by vanishing tangential electric and magnetic fields at these surfaces, respectively [30]. The effective medium parameters of the periodic structure are extracted from the scattering parameters by using the Nicolson-Ross-Weir technique (NRW) [31]. The effective electrical permittivity, ε_{eff}, magnetic permeability, μ_{eff}, and refractive index, n, are computed by Equations (1)–(3):

$$Z = \sqrt{\frac{(1 + S_{11})^2 - S_{21}^2}{(1 - S_{11})^2 - S_{21}^2}} \tag{1}$$

$$n = \frac{j}{k_o d} \ln \left(\frac{S_{21}}{1 - S_{11} \dfrac{z - 1}{z + 1}} \right) \tag{2}$$

$$\varepsilon_{eff} = \frac{n}{z}; \quad \mu_{eff} = nz \tag{3}$$

where Z, d, and k_o represent the impedance, thickness of the metamaterial, and free space wave number, respectively. Constitutive parameters of the SRR unit cell are demonstrated in Figure 2. The designed unit cell exhibits left-handed metamaterial characteristics between 3 GHz and 6.2 GHz. Since constitutive parameters are negative at 5 GHz, this structure can be used as a negative refractive index metamaterial at this frequency. An array consisting of the above mentioned unit cell is used to create the metasurface in an all-textile antenna operating at 5 GHz.

2.2. All-Textile Metasurface Antenna

A circular patch antenna with 11.4 mm radius (r) is designed on a polyester substrate with 4 mm thickness. The width and length of the ground plane are 50 mm and 75 mm, respectively. By using washable polyester as the dielectric and washable E-threads as the conductor, a washable all-textile antenna is made. The all-textile circular patch antenna is shown in Figure 3(a). The circular patch is positioned at the center of the rectangular polyester. The antenna is fed by a 50 Ω coaxial line. The feeding position is shifted $r/2$ from the center of the circular patch to obtain resonance at 5 GHz. By $r/2$ shift of the feed position from the patch center, the resonance frequency of the antenna is lowered to 5 GHz from 11.36 GHz without enlarging the physical size of the antenna [32].

Square SRRs are arranged to form a linear array of 4×1 and 4×2 elements. SRR arrays are placed to both sides of the circular patch along y-axis, and metasurface of the antenna is formed. All-textile metasurface antennas with 4×1 and 4×2 linear arrays of SRRs are demonstrated in Figure 3(b)
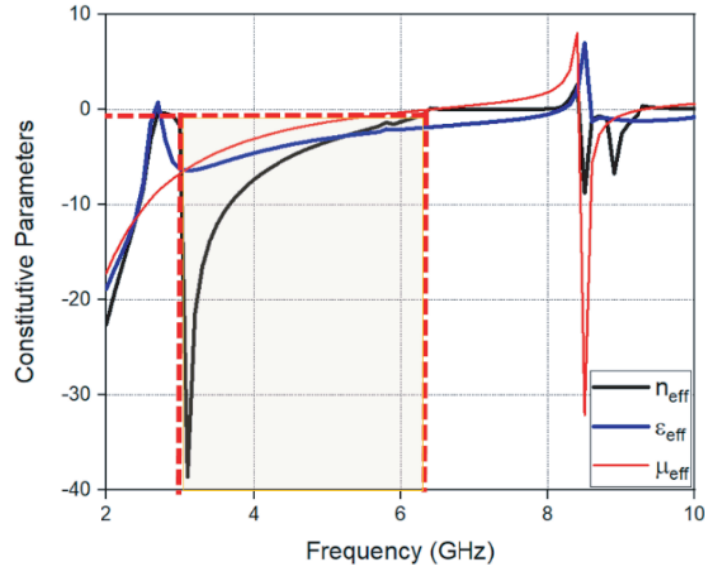
Figure 2. Constitutive parameters of the SRR unit cell.

(a)   (b)   (c)
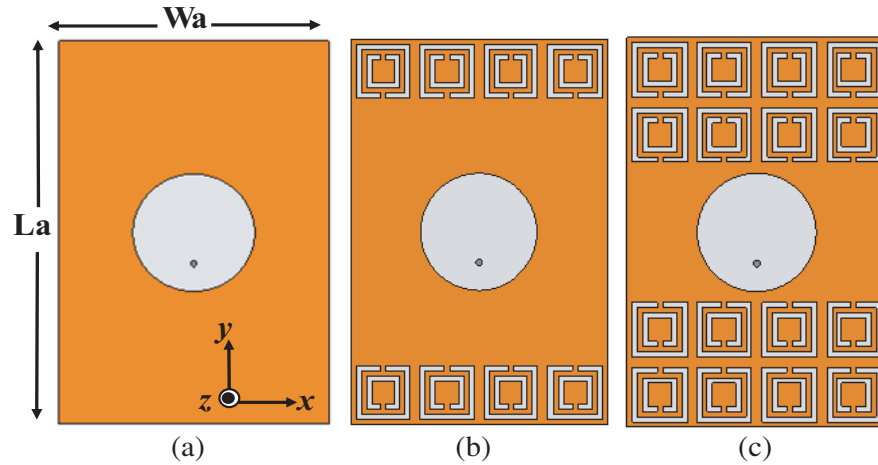
Figure 3. All-textile antennas. (a) Circular patch antenna. (b) Metasurface antenna with 4×1 linear array of SRRs. (c) Metasurface antenna with 4×2 linear array of SRRs.

and 3(c), respectively. The SRR cells have their gaps facing towards the circular patch to provide the required electrical field distribution of the cell.

3. PERFORMANCE ANALYSIS OF ALL-TEXTILE METASURFACE ANTENNA

The metasurface all-textile antennas that have been constructed by implanting SRR metamaterial arrays on the patch plane are designed to resonate at 5 GHz. The reflection coefficient variation of all-textile antennas is given in Figure 4 as the function of frequency. The bandwidth of the circular patch is 0.68 GHz which is equivalent to 13.6% band. The bandwidth increases about 4.6% in the antenna with 4×2 linear array of SRRs. Gain patterns of all-textile antennas at 5 GHz are given in Figure 5. As seen in Figure 5, creating an SRR array on the patch antenna increases the gain. 0.27 dB and 2.62 dB increases in gain are observed with 4×1 and 4×2 linear arrays of SRRs, respectively.
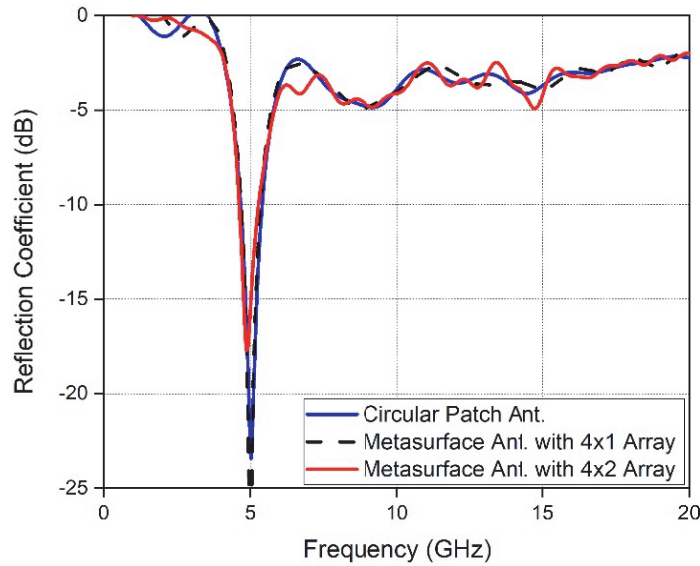
Figure 4. Reflection coefficient variation of all-textile antennas.
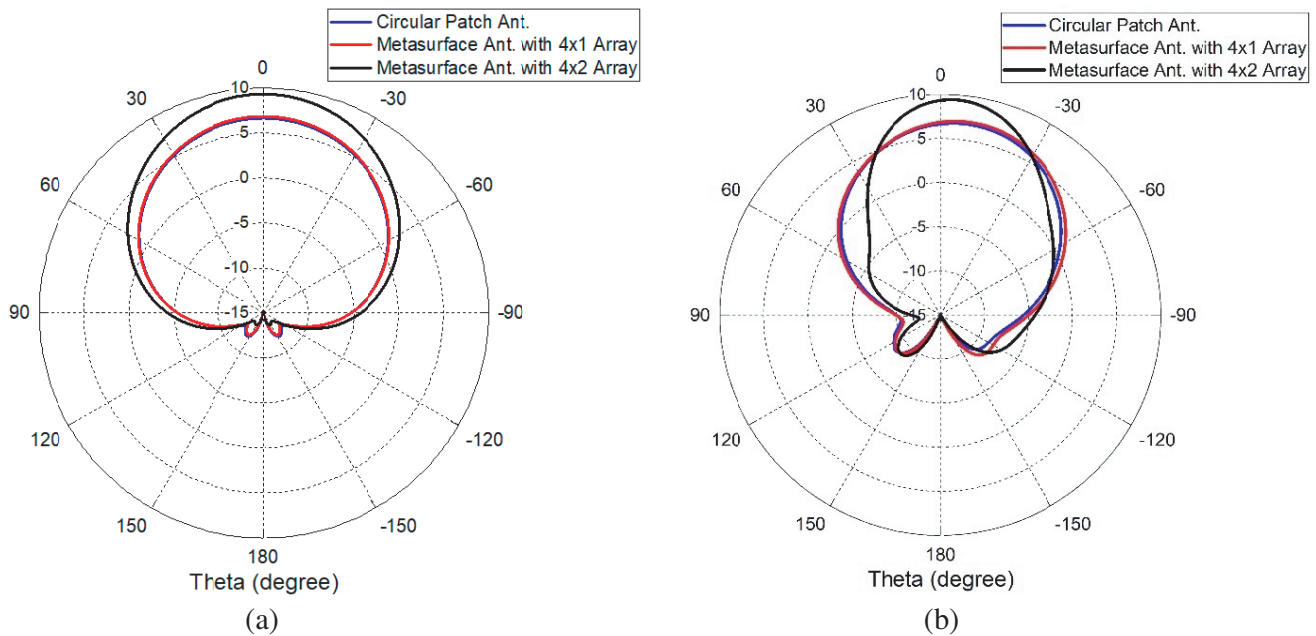
Figure 5. Gain patterns of all-textile antennas. (a) $\varnothing = 0°$ plane. (b) $\varnothing = 90°$ plane.

3.1. On-Body Performance

On-body antennas may be used on moving parts of the clothes that may be subject to bending. Besides, they may be used on conformal surfaces, such as the upper chest or arm. Bending the antenna to follow body movements may impair the performance of the textile antenna. Therefore, the performance of antennas should also be analyzed on conformal surfaces. On-body analysis is carried out by bending the antenna over a cylindrical surface that demonstrates the upper arm region. The arm radius is chosen as $R = 50$ mm. Thus, planar all-textile antennas are bended vertically and horizontally on a cylindrical surface with radius 50 mm as shown in Figure 6.

Reflection coefficient variation of the horizontally and vertically bended antennas is given in
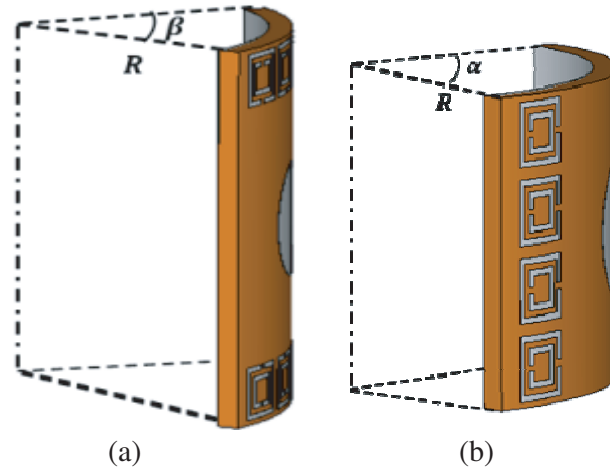
Figure 6. Metasurface all-textile antenna with 4×1 metamaterial array bended on a cylindrical surface. (a) Vertical bending. (b) Horizontal bending.
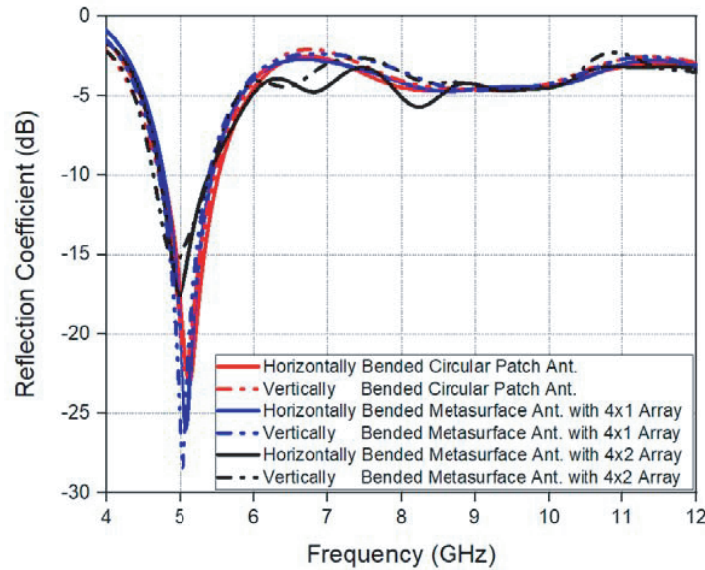
Figure 7. Reflection coefficient variation for horizontally and vertically bended ($R = 50\,\text{mm}$) all-textile antennas.

Figure 7. It is observed that the resonance frequency does not change much with bending of the antenna. There is a slight increase in the S_{11} level due to the bending. The normalized gain patterns of bended antennas are exhibited in Figure 8. Antennas bended horizontally and vertically on a $R = 50\,\text{mm}$ cylindrical surface exhibit similar radiation pattern characteristics in $\text{Ø} = 0°$ plane. However, the beams of the horizontally bended antennas widen in $\text{Ø} = 90°$ plane. This is an expected result since the curvature of the horizontally bended antenna is more than vertically bended one ($\alpha > \beta$). Bending the antenna vertically on the upper arm reduces the antenna gain about $0.91\,\text{dB}$ for the circular patch, whereas the reduction is $0.8\,\text{dB}$ and $1.09\,\text{dB}$ for the metasurface antennas with 4×1 and 4×2 linear arrays of SRRs, respectively. The gain decreases more in horizontally bended antennas. Efficiency and gain values of planar and bended all-textile antennas are compared in Table 1.
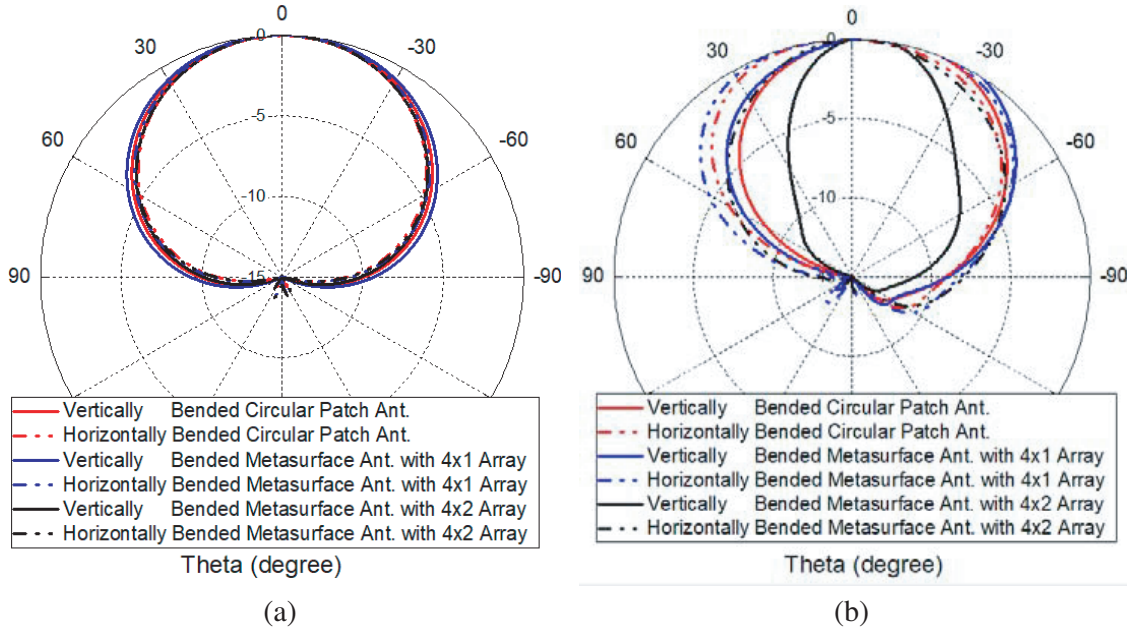
Figure 8. Normalized gain patterns of vertically and horizontally bended all-textile antennas. (a) $\emptyset = 0°$ plane. (b) $\emptyset = 90°$ plane.

Table 1. Efficiency and gain values of planar and curved all-textile antennas.

Type	Efficiency (%)			Gain (dBi)		
	Planar	Vertically Bended	Horizontally Bended	Planar	Vertically Bended	Horizontally Bended
Circular Patch Ant.	78.15	77	72.1	6.81	5.9	5.16
Metasurface Ant. with 4 × 1 Array	83.8	87	81	7.01	6.21	5.25
Metasurface Ant. with 4 × 2 Array	94.5	93.8	97	9.43	8.34	6.78

4. FABRICATION AND EXPERIMENTAL CHARACTERIZATION

The dielectric layer of the all-textile antennas consists of a polyester fabric with a thickness of 4 mm. Each layer of the polyester fabric used in production has 0.16 mm thickness. Polyester fabric layers of 50 mm × 75 mm are cut with a laser machine as shown in Figure 9(a). Using a laser cutting machine instead of cutting the polyester fabric with scissors and similar tools eliminates the risk of loose threads that may occur around the fabric. The polyester layers are bonded with an 80-degree temperature resistant, silicone-free spray fabric adhesive, which is resistant to washing in the washing machine. Since the materials used in the antenna design are washable, choosing the adhesive with this feature protects the original washable design. The dielectric base of 4 mm thickness is obtained by combining 25 pieces of 100% polyester fabric.

All-textile metasurface antennas with SRR arrays on both sides of the circular patch are produced using an embroidery machine that is commonly used in textile manufacturing. Silver-plated highly conductive E-thread is used. The fabrication steps of the conductive parts are demonstrated in Figure 9(b). The substrate is bonded with the lower and upper conductive layers with the spray fabric adhesive. To solder 50 Ω SMA connector to the antennas for coaxial line feeding, holes that have the
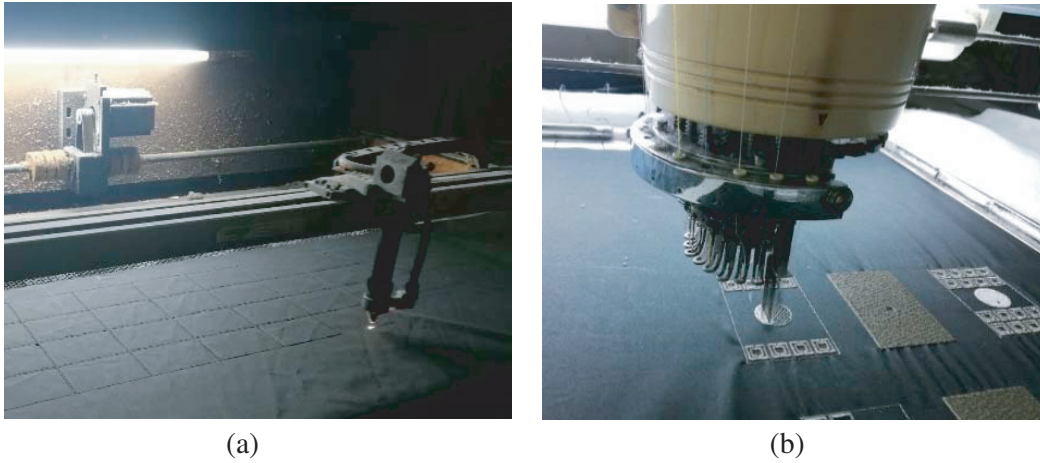
Figure 9. Fabrication steps of the all-textile antennas. (a) Laser cutting of polyester dielectric layers. (b) Embroidery of the conductive parts using embroidery machine.
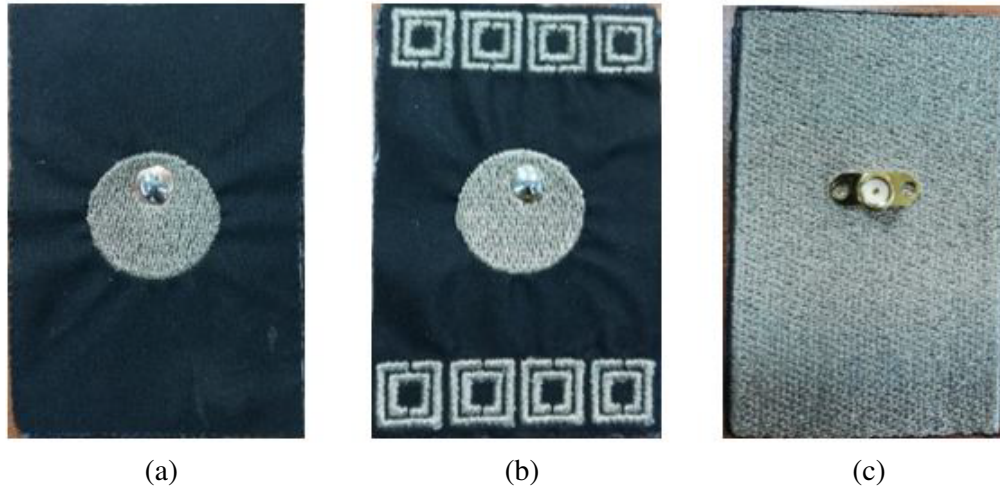
Figure 10. Fabricated prototype of all-textile antennas. (a) Top view of circular patch antenna. (b) Top view of metasurface antenna with 4×1 linear SRR arrays. (c) Bottom view of all-textile antennas.

pin and outer conductor radius are drilled. Top view of the fabricated circular patch antenna prototype is given in Figure 10(a). The pin of the connecter is soldered to the embroidered patch. A small circular copper plate is used as the base for the solder. Top view of the fabricated metasurface antenna with 4×1 linear arrays of SRRs is shown in Figure 10(b). SRR metamaterial unit cells in array form are embroidered on lateral sides of the patch. The embroidered ground plane of the all-textile antennas is given in Figure 10(c).

Antennas are measured within the angular range of $-90° \leq \theta \leq 90°$. Anritsu MS4644A 2-port network analyzer is used in the measurements. The transmitting antenna used in the measurement is a broadband horn antenna operating in the 0.8 GHz–18 GHz frequency band. Measured reflection coefficient variation of the antennas is given in Figure 11 together with simulation results. In Figure 11, there is a difference in resonance frequency of the measured and simulated antennas. This is attributed to the thickness differences of the substrates. The layers are bonded to each other to form 4 mm thickness. Air molecules that remained within the adhesive altered the thickness of the substrate and shifted the resonant frequency. Besides, although the stroke frequency of the E-threads was very high during the processing of the E-thread in the embroidery machine (e.g., 6467 strokes per minute), minimal air gaps
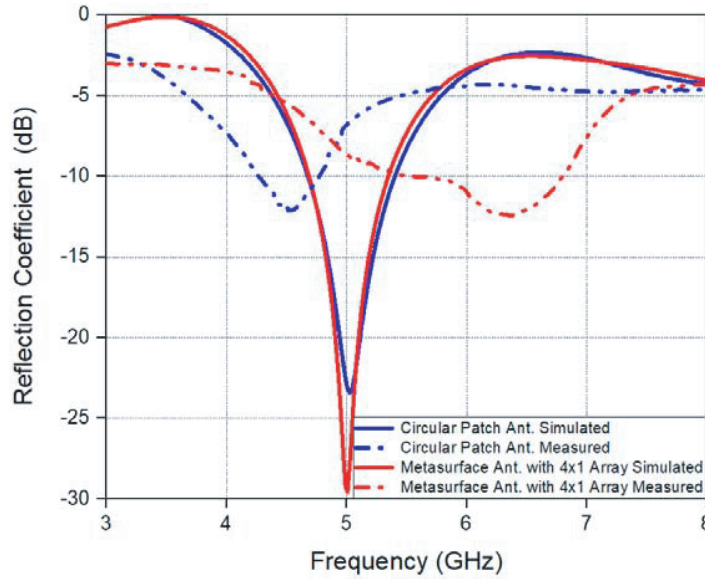
Figure 11. Measured reflection coefficient variation of the fabricated all-textile antennas.

may have been formed in the conductive parts of the antennas. The measured S_{11} variation of the antennas shows that the measured all-textile circular patch antenna operates in the 4.2 GHz–4.8 GHz frequency band. The antenna has a bandwidth of 0.6 GHz (13.3% BW). The all-textile metasurface antenna with a 4×1 linear SRR array has measured S_{11} lower than -10 dB within 5.8 GHz–6.8 GHz frequency band which is equivalent to 1 GHz bandwidth (15.8% BW).

Measured radiation patterns of the fabricated all-textile antennas are given in Figure 12. Normalized patterns at 4, 4.25, and 4.5 GHz are exhibited for the all-textile circular patch antenna. Although main lobe direction is at $\theta = 0°$ at 4 and 4.25 GHz, it shifts to $\theta = 40°$ at 4.5 GHz. Measured radiation patterns of the fabricated all-textile metasurface antenna with 4×1 linear SRR arrays is given in Figure 12(b). Since S_{11} of this antenna has lower value than -10 dB in the 5.8 GHz–6.8 GHz frequency band, normalized radiation patterns at 5.75, 6, 6.25, and 6.5 GHz are demonstrated. Angular shift observed in the measured main beam direction was not observed in the simulations. This shift is attributed to the difficulties experienced in the production process. The gain values obtained due to the problems arising from production are quite low compared to the values obtained in the simulation results. However, gain patterns show that metasurface antenna with a 4×1 linear SRR array increases the antenna gain by 24.75% compared to circular patch antenna. In Table 2, the proposed all-textile
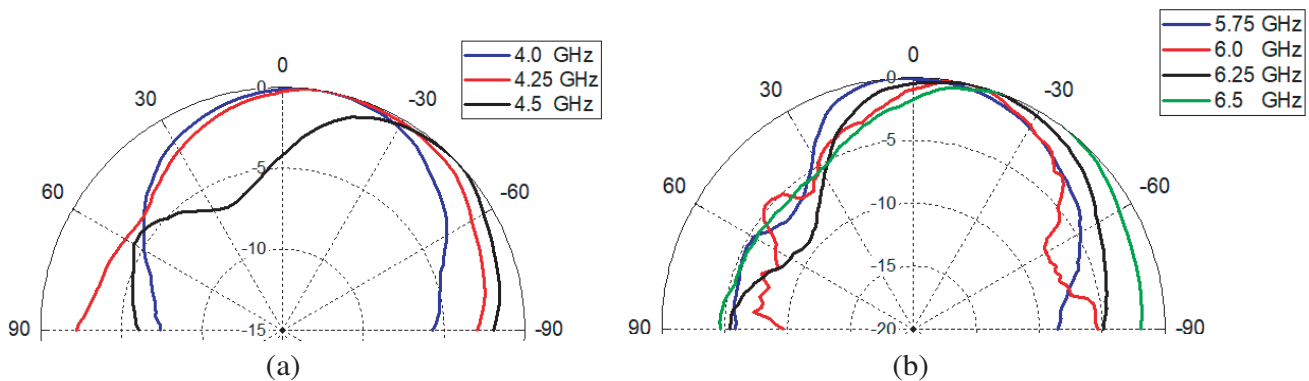
Figure 12. Measured copolarized radiation patterns of the fabricated all-textile antennas. (a) Circular patch antenna. (b) Metasurface antenna with 4×1 linear SRR array.

Table 2. Comparison of proposed all-textile metasurface antenna with recent all-textile antennas that consists of metamaterial.

Reference	Structure	Size (mm × mm)	f_0 (GHz)	Gain (dBi)	Efficiency (%)
[1]	All-Textile Metamaterial-Inspired Antenna	50 × 50	5.14	6.6	75
[11]	Wearable PIPA with an All-Textile Metasurface Antenna	42 × 28	5.5	6.70*	77*
[25]	Metamaterial-Inspired SIW Textile Antenna	74.7 × 47.7	2.45	5.42	76
[26]	Embroidered Metamaterial Antenna	85 × 70	2.45	7.81	80.4
This Work	All-Textile Metasurface Antenna with 4 × 2 Metamaterial Array	50 × 75	5	9.43	94.5

*Values are extracted from the plots.

metasurface antenna with 4 × 2 linear arrays of metamaterial is compared with recent all-textile antennas that consist of metamaterial. The results belong to simulated antennas. As shown in the table, the proposed design has higher gain and efficiency than other all-textile antennas that consist of metamaterial structure.

5. SPECIFIC ABSORPTION RATE ANALYSIS

An arm phantom was formed by bending the metasurface antenna with 4 × 2 linear SRR arrays on a cylindrical surface with an average arm diameter of $R = 50$ mm. Since maximum SAR is very close to the epidermis and dermis layers of the skin, a region of the upper male arm is used in the analysis. Problem space is exhibited in Figure 13 with tissue layers of the arm. From the outermost layer to the inner side, the arm phantom consists of skin with 2 mm thickness, fat with 15 mm thickness, muscle with 20 mm thickness, and bone tissue with 13 mm radius [33]. The arm phantom has 150 mm length. SAR values are evaluated for horizontally and vertically bended antenna using CST Microwave Studio by implementing time-domain Finite Integration Technique (FIT). The antenna is centered to the arm phantom during the SAR analysis. The antenna is positioned at a distance of 5 mm away from the skin layer.
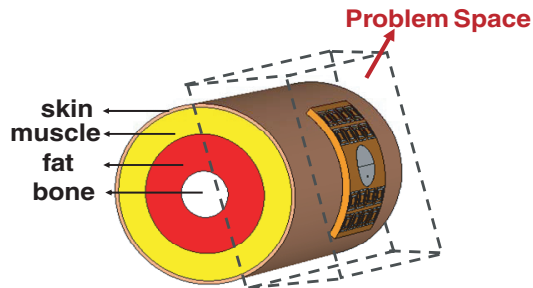
Figure 13. Arm phantom model and problem space representation of the analysis.

Table 3. Electrical properties of the tissues in arm phantom.

Tissue	Conductivity (S/m)	Relative Permittivity	Loss Tangent	Density (kg/m^3)
Skin	3.0608	35.774	0.3076	1109
Fat	0.24222	5.0291	0.17315	911
Muscle	4.0448	49.54	0.29353	1090
Bone	0.96228	10.04	0.34459	1908

The electrical properties of the tissues in arm phantom at 5 GHz are shown in Table 3 [34]. The antenna is excited with an input power ranging from 20 dBm to 30 dBm. SAR values were studied on 10 g tissue. The maximum SAR values calculated for the arm phantom are given in Figure 14 as the function of input power. Blue and red solid lines correspond to vertically and horizontally placement of the antennas on arm phantom. The ICNIRP recommendations and EU Council Recommendation 1999/519/EC on exposure limits to electromagnetic fields presented that the SAR value limitation in whole body average should not exceed 2 W/kg per 10 g of tissue [35]. The spatial peak SAR variation of the proposed metasurface antenna meets current ICNIRP's SAR limit regulations for all input powers up to 1000 mW. The maximum SAR remains within the skin layer and well below the limits in the designed arm models.
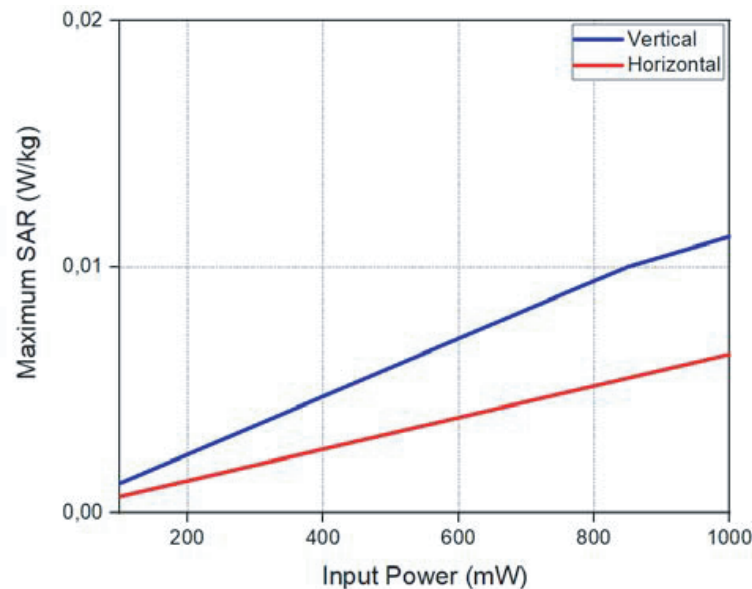
Figure 14. Maximum SAR variation of the vertically and horizontally located all-textile antenna as the function of input power.

6. CONCLUSIONS

With the development of wireless communication systems, wearable antennas have become an inevitable component of applications such as remote healthcare, emergency services, physical education, public security, and location tracking. For these applications, light weight and low profile antennas with high gain and low SAR value are needed. Mostly the antennas are embedded in garments. Thus, performance of the antenna should be considered on-body, as well. In this work, novel, all-textile, washable metasurface antennas for on-body applications are proposed. Two different metamaterial arrays consisting of SRR unit cells are designed and placed on lateral sides of the circular patch. It is observed that the metasurface antenna with linear arrays of SRR metamaterial cells significantly

increases the antenna gain and efficiency compared to traditional circular patch antenna. Performance of the proposed metasurface antenna is verified on conformal surfaces, as well. The electromagnetic power absorption properties of the antenna are numerically evaluated using an upper arm phantom. The SAR value remains well below the limits for input powers up to 30 dBm, making the antennas suitable for use as a body antenna. The antennas are fabricated with standard off-the-shelf parts using standard textile manufacturing technique, namely embroidery machine. This paper, to the best of our knowledge, is the first in using E-tread for the fabrication of metasurface antenna. With its low cost, high gain, and efficiency features, the proposed metasurface antenna can be used in wireless body area networks and 5G applications.

REFERENCES

1. Yan, S., P. J. Soh, and G. A. E. Vandenbosch, "Compact all-textile dual-band antenna loaded with metamaterial-inspired structure," *IEEE Antennas and Wireless Propagation Letters*, Vol. 14, 1486–1489, 2015.

2. Moro, R., S. Agneessens, H. Rogier, A. Dierck, and M. Bozzi, "Textile microwave components in substrate integrated waveguide technology," *IEEE Transactions on Microwave Theory and Techniques*, Vol. 63, No. 2, 422–432, Feb. 2015.

3. Joshi, R., et al., "Dual-band, dual-sense textile antenna with AMC backing for localization using GPS and WBAN/WLAN," *IEEE Access*, Vol. 8, 89468–89478, 2020.

4. Tak, J. and J. Choi, "An all-textile Louis Vuitton logo antenna," *IEEE Antennas and Wireless Propagation Letters*, Vol. 14, 1211–1214, 2015.

5. Locher, I., M. Klemm, T. Kirstein, and G. Troster, "Design and characterization of purely textile patch antennas," *IEEE Trans. Adv. Packag.*, Vol. 29, No. 4, 777–788, Nov. 2006.

6. May, W. E., I. Sfar, J.-M. Ribero, and L. Osman, "A millimeter-wave textile antenna loaded with EBG structures for 5G and IoT applications," *2019 IEEE 19th Mediterranean Microwave Symposium (MMS)*, 1–4, 2019.

7. Ouyang, Y. and W. J. Chappell, "High frequency properties of electro-textiles for wearable antenna applications," *IEEE Transactions on Antennas and Propagation*, Vol. 56, No. 2, 381–389, Feb. 2008.

8. Lopes, C., C. Loss, R. Salvado, P. Pinho, S. Agneeessens, and H. Rogier, "Development of substrate integrated waveguides with textile materials by manual manufacturing techniques," *Proceedings of the 2nd Int. Electron. Conf. Sens. Appl.*, S3004, 2014.

9. Stoppa, M. and A. Chiolerio, "Wearable electronics and smart textiles: A critical review," *Sensors*, Vol. 14, 11957–11992, 2014.

10. Mashaghba, H. A., et al., "Bending assessment of dual-band split ring-shaped and bar slotted all-textile antenna for off-body WBAN/WLAN and 5G applications," *2020 2nd International Conference on Broadband Communications, Wireless Sensors and Powering (BCWSP)*, 2020.

11. Gao, G., C. Yang, B. Hu, R. Zhang, and S. Wang, "A wearable PIFA with an all-textile metasurface for 5 GHz WBAN applications," *IEEE Antennas and Wireless Propagation Letters*, Vol. 18, No. 2, 288–292, Feb. 2019.

12. Antenna, P., M. N. Ammal, B. Ramachandran, P. H. Rao, and D. N. Kumar, "5 GHz WLAN band-notched UWB symmetrical slotted PI-notched parasitic planar," *2013 International Conference on Advances in Computing, Communications and Informatics (ICACCI)*, 338–342, 2013.

13. Sharma, D., S. K. Dubey, and V. N. Ojha, "Wearable antenna for millimeter wave 5G communications," *2018 IEEE Indian Conference on Antennas and Propogation (InCAP)*, 2018.

14. Zhong, J., A. Kiourti, T. Sebastian, Y. Bayram, and J. L. Volakis, "Conformal load-bearing spiral antenna on conductive textile threads," *IEEE Antennas and Wireless Propagation Letters*, Vol. 16, 230–233, 2017.

15. Celenk, E. and N. T. Tokan, "All-textile on-body antenna for military applications," *IEEE Antennas and Wireless Propagation Letters*, Early Acess Article, 2022.

16. Ahmed, A., M. R. Robel, and W. S. T. Rowe, "Dual-band two-sided beam generation utilizing an EBG-based periodically modulated metasurface," *IEEE Transactions on Antennas and Propagation*, Vol. 68, No. 4, 3307–3312, Apr. 2020.

17. Veselago, V. G., "The electrodynamics of substances with simultaneously negative values of ε and μ," *Soviet Physics Uspekhi*, Vol. 10, 509–514, 1968.

18. Smith, W. J., D. C. Padilla, S. C. Vier, C. Nemat-Nasser, and S. Schultz, "Composite medium with simultaneously negative permeability and permittivity," *Physical Review Letters*, Vol. 84, 4184–4187, 2000.

19. Valentine, J., S. Zhang, T. Zentgraf, E. Ulin-Avila, D. A. Genov, G. Bartal, and X. Zhang, "Three-dimensional optical metamaterial with a negative refractive index," *Nature*, Vol. 455, 376–379, 2008.

20. Wahidi, M. S., M. I. Khan, F. A. Tahir, and H. Rmili, "Multifunctional single layer metasurface based on hexagonal split ring resonator," *IEEE Access*, Vol. 8, 28054–28063, 2020.

21. Syihabuddin, B., M. R. Effendi, and A. Munir, "Characterization of X-band wave absorber made of SRR-based metasurface," *2019 IEEE Conference on Antenna Measurements* & *Applications (CAMA)*, 1–4, 2019.

22. Aznabet, M., et al., "Wave propagation properties in stacked SRR/CSRR metasurfaces at microwave frequencies," *2009 Mediterrannean Microwave Symposium (MMS)*, 1–4, 2009.

23. Nguyen, T. K., S. K. Patel, S. Lavadiya, J. Parmar, and C. D. Bui, "Design and fabrication of multiband reconfigurable copper and liquid multiple complementary split-ring resonator based patch antenna," *Waves in Random and Complex Media*, 1–24, 2022.

24. Lavadiya, S. P., S. K. Patel, and R. Maria, "High gain and frequency reconfigurable copper and liquid metamaterial tooth based microstrip patch antenna," *AEU — International Journal of Electronics and Communications*, Vol. 137, 153799, 2021.

25. Lajevardi, M. E. and M. Kamyab, "Ultraminiaturized metamaterial-inspired SIW textile antenna for off-body applications," *IEEE Antennas and Wireless Propagation Letters*, Vol. 16, 3155–3158, 2017.

26. Gil, I., R. Seager, and R. Fernández-García, "Embroidered metamaterial antenna for optimized performance on wearable applications," *Phys. Status Solidi (a)*, Vol. 215, No. 21, Art. No. 1800377, 2018.

27. Hong, Y., J. Tak, and J. Choi, "An all textile SIW cavity-backed circular ring slot antenna for WBAN applications," *IEEE Antennas and Wireless Propagation Letters*, Vol. 15, 1995–1999, 2016.

28. Gao, G., C. Yang, B. Hu, R. Zhang, and S. Wang, "A wide-bandwidth wearable all-textile PIFA with dual resonance modes for 5 GHz WLAN applications," *IEEE Transactions on Antennas and Propagation*, Vol. 67, No. 6, 4206–4211, Jun. 2019.

29. Madeira, "HC conductive Treads Switch on the Magic," 6, 2021.

30. Dogan, E., E. Unal, and D. Kapusuz, "New generation WIMAX antenna based on metamaterial superstrate," *Optoelectronics and Advanced Materials — Rapid Communications*, 1002–1010, 2013.

31. Dogan, E., E. Unal, D. Kapusuz, M. Karaaslan, and C. Sabah, "Microstrip patch antenna covered with left handed metamaterial," *ACES Journal*, Vol. 28, No. 10, 9999–1004, 2013.

32. Çelenk, E. and N. T. Tokan, "All-textile, washable metasurface antenna for WBAN/WLAN and mid-band 5G applications," *2021 13th International Conference on Electrical and Electronics Engineering (ELECO)*, 305–309, 2021.

33. Hu, B., G. Gao, L. He, X. Cong, and J. Zhao, "Bending and on-arm effects on a wearable antenna for 2.45 GHz body area network," *IEEE Antennas and Wireless Propagation Letters*, Vol. 15, 378–381, 2016.

34. Gabriel, C., "A compilation of the dielectric properties of body tissues at RF and microwave frequencies," *Radio Freq. Radiat. Division*, Brooks Air Force Base, San Antonio, TX, USA, Tech. Rep. AL/OE-TR-1996-0037, 1996.

35. Commission Implementing Decision (EU) 2016/537, *Official J. Eur.*, Apr. 5, 2016.